Organic Electronics 49 (2017) 212–217

Contents lists available at ScienceDirect

Organic Electronics

journal homepage: www.elsevier.com/locate/orgel

# Exploring the ultrasonic nozzle spray-coating technique for the fabrication of solution-processed organic electronics

Singu Han [a, 1], Heejeong Jeong [a, 1], Hayeong Jang [a], Seolhee Baek [a], Se Hyun Kim [b, **], Hwa Sung Lee [a, *]

[a] Department of Chemical & Biological Engineering, Hanbat National University, Daejeon 305-719, Republic of Korea
[b] Department of Nano, Medical and Polymer Materials, Yeungnam University, Gyeongsan 712-749, Republic of Korea

ARTICLE INFO

*Article history:*
Received 22 May 2017
Received in revised form
20 June 2017
Accepted 26 June 2017
Available online 27 June 2017

*Keywords:*
Ultrasonic nozzle spray
Solution process
Organic electronics
Conducting polymer
PEDOT:PSS

ABSTRACT

The ultrasonic nozzle (US) spray method was investigated for its utility in fabricating organic electrodes composed of poly(3,4-ethylenedioxythiophene):poly(styrenesulfonate) (PEDOT:PSS), a standard conductive polymer material used to produce large-area low-cost OFETs. The US spray technique involves generating a solution spray by first passing the solution through a head and nozzle subjected to ultrasonic vibrations that induce atomization. This method is advantageous in that the resulting spray comprises extremely small solution droplets a few micrometers in diameter, unlike the spray produced using conventional air spray methods. The PEDOT:PSS US solution spraying process was optimized by controlling the flow rate of the $N_2$ carrier gas and the substrate temperature while monitoring the quality of the resulting PEDOT:PSS electrode films. The pentacene field-effect transistors prepared using the US spray method displayed a maximum field-effect mobility of 0.47 $cm^2V^{-1}s^{-1}$ (with an average value of 0.31 $cm^2V^{-1}s^{-1}$), 35% better than the mobilities achieved using the conventional air spray method. In addition, the device-to-device reproducibility was improved, as indicated by a decrease in the standard deviation of the mobility values from 30% for the air spray devices to 24% for the US spray devices. These results indicated that the US spray technique is efficient and superior to the conventional air spray method for the development of low-cost large-area organic electronics.



## 1. Introduction

In recent years, organic field-effect transistors (OFETs) have been intensively developed for use in various electronic devices, such as displays, antennas, and sensors [1–5]. Most processes used to fabricate OFETs are either vacuum deposition or solution processes [6–10]. Vacuum deposition processes can produce high-performance OFETs, although these processes are expensive, require high-vacuum conditions, and are difficult to apply to large-area fabrication methods [6,7]. Solution processes are advantageous for producing low-cost large-area OFETs, although it is difficult to achieve the reproducibility and uniformity of their electrical performances [8–10]. Large-area low-cost fabrication processes rely on a variety of solution process printing technologies, such as inkjet printing, nanoimprinting, screen printing, and roll-to-roll printing [11–17]. These solution printing techniques are difficult to optimize, and optimal process conditions tend to be relatively high in cost [11–17]. These processes are, however, suitable for producing relatively precise and expensive organic electronics. Other printing methods are needed for the facile and rapid production of large-area low-priced organic electronics.

The air spray printing method is a solution process technology commonly used to manufacture low-cost organic thin films because among the various OFET solution manufacturing processes, air spray printing provides the most uniform coating quality over large areas [18–24]. In 2010, Abdellah group systematically studied organic photovoltaic layer deposition processes based on the air spray printing of a blend of regioregular poly(3-hexylthiophene-2,5-diyl) (P3HT) and [6,6]-phenyl C61 butyric acid methyl ester (PCBM) as the donor and acceptor materials, respectively [23]. They successfully fabricated air-sprayed P3HT-FETs, although the electrical performances were low, with a field-effect mobility of

* Corresponding author.
** Corresponding author.
*E-mail addresses:* shkim97@yu.ac.kr (S.H. Kim), hlee@hanbat.ac.kr (H.S. Lee).
[1] S. Han and H. Jeong contributed equally to this work.

http://dx.doi.org/10.1016/j.orgel.2017.06.061
1566-1199/

$1.02\times10^{-4}$ $cm^2V^{-1}s^{-1}$ [23]. Kim and Noh groups reported the fabrication of OFETs and complementary inverters using the air spray printing of small molecule organic semiconductors and P3HT in 2013 [24]. They obtained highly crystalline organic semiconductors using the spray printing method and reported that the organic electronic devices yielded excellent electrical performances [24]. The spray printing technique unfortunately does not provide uniform surface coatings with high precision because the diameters of the solution droplets ejected from the nozzle range from 50 to 1000 μm. Solid particle dispersions, in particular, produce nonuniform films because the solid dispersion degree can change during the coating process. Recently, the ultrasonic nozzle (US) spray method was introduced to complement the air spray printing method [25–28]. The US technique involves coating equipment designed to apply ultrasonic vibrations to the nozzle from which the solution is sprayed. The solution is then discharged in very small droplets with diameters of 2–5 μm, which is possible to produce microscopically uniform organic films compared with the conventional spray coating method [26–29]. The uniform solution composition and spraying conditions remain constant over time because the mechanical ultrasonic vibrations of the nozzle tend to preserve the dispersion stability. The uniformity of the coated films obtained using solid-dispersed solutions tends to be superior to those obtained using the air spray method. In additional, the operational principle of the US spray gives the several advantages, such as the minimization of nozzle clogging problem or solution waste, the controllabilities of low velocity or low flux spray, and the process stability of spray conditions.

In this study, the US spray method was used to fabricate organic electrodes composed of poly(3,4-ethylenedioxythiophene):poly(styrenesulfonate) (PEDOT:PSS), a conductive polymer material commonly used to fabricate large-area low-cost OFETs. In order to investigate the optimal US spray conditions, the flow rate of the $N_2$ carrier gas and the substrate temperature. The active layer of the OFET devices was prepared from pentacene, a standard organic semiconducting material, to enable a direct comparison to the literature values [21,30–32]. The pentacene FETs prepared using the US spray method displayed a maximum field-effect mobility of 0.47 $cm^2V^{-1}s^{-1}$ (with an average value of 0.31 $cm^2V^{-1}s^{-1}$), representing a 35% improvement over the values obtained using the conventional air spray method. The device-to-device reproducibility was also improved, as indicated by the decrease in the standard deviation of the mobility from 30% for the air spray devices to 24% for the US spray devices. These results revealed that the US spray technique efficiently provided uniform organic active layers, electrodes, or dielectric layers, the electrical performances of which are significantly affected by the film quality.

## 2. Experimental section

### 2.1. Materials and sample preparation

A highly doped n-type silicon wafer with a natural oxide layer was used as the substrate and the gate electrode. Prior to spin-coating the PVP dielectric layer, the wafer was washed and sonicated several times with copious amounts of tetrahydrofuran, toluene, and ethanol. A 350 nm polymer gate dielectric (capacitance = 11.3 nF $cm^{-2}$) was fabricated by spin-casting a 10 wt% poly-4-vinylphenol (PVP, $M_w = 20\ kg\ mol^{-1}$, Sigma-Aldrich) solution onto a silicon wafer, which acted as a gate electrode. PVP and the cross-linking agent poly(melamine-co-formaldehyde) (PMF, Sigma-Aldrich) were dissolved in a molar ratio of 1:1 in propylene glycol methyl ether acetate (PGMEA, Sigma-Aldrich). The PVP film was subsequently cross-linked over 2 h at 200 °C in a vacuum oven. The conducting poly(3,4-ethylenedioxythiophene):poly(styrenesulfonate) (PEDOT:PSS) in water (Baytron P, from Bayer AG) was used as the ink to pattern the source and drain electrodes. The patterned electrodes were patterned by spraying the PEDOT:PSS ink onto the PVP dielectrics using the US (N180, Noanix) system or the air spray (Creamy(K)3A, Kinki) system, with nitrogen ($N_2$, 99.9%) as the carrier gas. The spray stream was delivered over a distance of 10 cm between the nozzle and the substrate through a metal mask with a channel length (L) and width (W) of 100 and 1000 μm, respectively. The 50 nm thick pentacene (Aldrich Chemical Co., no purification) films were evaporated from a quartz crucible at a rate of 0.2 Å/s and at a substrate temperature of 30 °C using an organic molecular beam deposition (OMBD) system under a base pressure of $10^{-7}$ Torr. The deposition rate, film thickness, and substrate temperature were recorded during deposition.

### 2.2. Characterization

The thicknesses of the PVP gate dielectric layers coated onto the Si substrate were measured using an alpha-step profilometer (Dektak 150, Veeco). The morphologies of the PVP, PEDOT:PSS, and pentacene films were obtained using atomic force microscopy (AFM, Digital Instruments Multimode) collected via tapping-mode AFM using a $SiN_x$ cantilever and Si tips (42 N/m and 320 kHz, tip radius: 10 nm). Data analysis was performed using the Nanoscope 5.30 software. The morphologies of the patterned PEDOT:PSS electrodes were characterized by optical microscopy (OM, Eclipse 80i, Nikon), field-emission scanning electron microscopy (SEM, Hitachi S-4200), and AFM. The current–voltage characteristics of the OFETs were examined by operating the devices under a negative applied gate bias. The source electrode was grounded and the drain electrode was negatively biased. The electrical parameters characterizing the pentacene-OFETs were obtained at room temperature using an HP4156A instrument in a dark environment under vacuum conditions ($10^{-4}$ Torr).

## 3. Results and discussion

A schematic diagram and photographic images of the US spray system used in our experiments are shown in Fig. 1. The US is a type of spray nozzle that applies high frequency mechanical vibrations produced by piezoelectric transducers to the nozzle tip to create

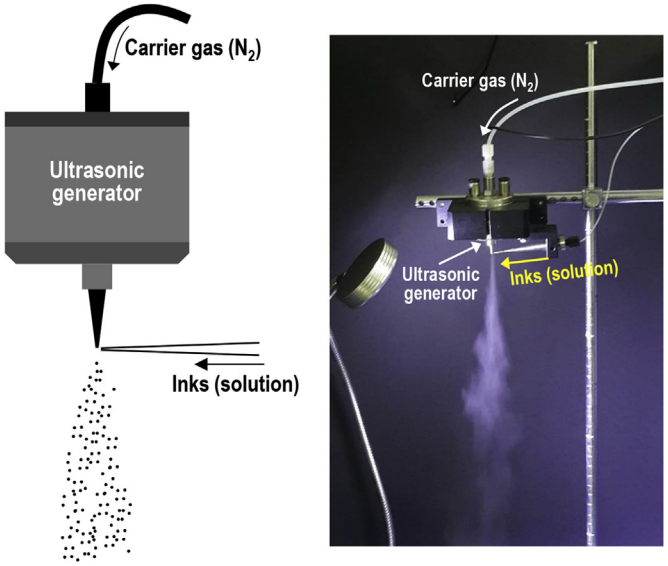


**Fig. 1.** Schematic diagram (**left**) and photograph (**right**) of the US spray system used in our experiments.

capillary waves within the liquid film. Once the amplitude of the capillary waves reaches a critical value, the waves become too tall to support themselves, and tiny droplets fall from the tip of each wave, thereby atomizing the feed solution. The oscillating US disintegrates the solution (ink) to form micron-sized droplets that are delivered in a spray onto the substrate surface. Unlike a conventional air (or air-nozzle) spray, the sprayed droplet size may be tuned by the ultrasonic frequency, and the droplets are very small compared with the droplets produced in an air spray system. In our system, the frequency of the ultrasonic generator and the injection volume of the solution were fixed at 180 kHz and 0.2 mL/min, respectively, and $N_2$ was used as the carrier gas.

Fig. 2 shows photographic images of the US spray streams produced under various supplied $N_2$ carrier gas flow rates. As shown in the figure, even in the absence of a carrier gas, the solution formed a fine spray due to the ultrasonic vibrations applied to the nozzle head, and the sprayed droplets moved downward due to the influence of gravity. However, in the absence of a carrier gas, the sprayed stream easily deformed, and a uniform coating could not be obtained. Carrier gas flow rates of 0.5 or 1.0 mL/min delivered the sprayed droplets directly to the substrate, and the film formed an even coating. A flow rate of 1.0 mL/min was found to be sufficiently strong and fast to reduce the solution spray range compared to the 0.5 mL/min flow rate; thus, the spray penetrated the gap between the mask and the substrate. Residues were, therefore, deposited in undesirable areas, forming inaccurate patterns. In this experiment, the PEDOT:PSS coating was applied using the US spraying process at an optimal flow rate of 0.5 mL/min.

Fig. 3 shows OM images of the patterned PEDOT:PSS electrodes prepared at various substrate temperatures using the US spray process. A shadow mask was used to pattern the source (S) and drain (D) electrodes. As shown in Fig. 3 (a), spraying the PEDOT:PSS solution onto the substrate at room temperature resulted in PEDOT:PSS residue between the mask and the substrate, in addition to the S/D electrode pattern. The solution sprayed at room temperature did not dry evenly after reaching the substrate, and the wet solution permeated the area between the substrate and the mask. The PEDOT:PSS droplets that reached the substrates heated to 40 °C (Fig. 3 (b)) or 60 °C (Fig. 3 (c)) dried, and the PEDOT:PSS residue produced by permeation through the mask/substrate gap decreased significantly. A substrate temperature of 80 °C, as shown in Fig. 3(d), produced undesired shapes on the periphery of the electrode pattern. This effect may have resulted from a dramatic reduction in the surface tension of the PEDOT:PSS solution due to the high substrate temperature. The low surface tension promoted penetration of the PEDOT:PSS solution into the gap between the mask and the substrate. Fig. 3(e) shows an image of the large-area PEDOT:PSS electrode patterns sprayed onto a PVP dielectric surface using the US spray system at the optimal substrate temperature of 60 °C. As shown in the figure, the PEDOT:PSS electrodes were uniformly and accurately patterned over the entire area. These results are highlighted in the inset images of Fig. 3(e).

The morphological properties of our pentacene-FET devices were characterized by analyzing the surfaces of each component layer using AFM, as shown in Fig. 4. The FET device structures formed from the deposited pentacene films and PEDOT:PSS S/D electrodes are shown in Fig. 4(a) and its inset image, which shows a bottom-gate top-contact transistor. Fig. 4(b) shows the morphology of a PVP dielectric surface spin-coated onto a silicon substrate. The surface structures of the PVP dielectric were characterized, revealing pinholes 1.5 nm in depth and 50–400 nm in diameter. The *rms* roughness of the PVP dielectric was 0.17 nm, not considering the pinholes, and the overall *rms* roughness, including the pinholes, was 0.36 nm, indicating a generally smooth surface. The presence of pinholes was not expected to significantly affect the properties of the polymer dielectrics, due to the vary small thickness portion of them compared to the 350 nm-thick PVP dielectric layer and their long roughness wavelength [33–36]. Fig. 4(c) shows the surface morphology of the PEDOT:PSS electrode coated using the US spray method onto the PVP dielectric. As shown in the figure, the film was uniform and had a smooth surface with an *rms* roughness of 1.3 nm. The morphologies of the pentacene films deposited onto the PEDOT:PSS electrode and the PVP dielectric are shown in Fig. 4(d) and (e), respectively. The films exhibited a dendritic structure; however, a pentacene grain formed on the PEDOT:PSS electrode appeared to be a mixture of small mounds or bumpy dendritic grain surfaces. The pentacene grains in the PEDOT:PSS electrode were 100–240 nm in size, whereas they were

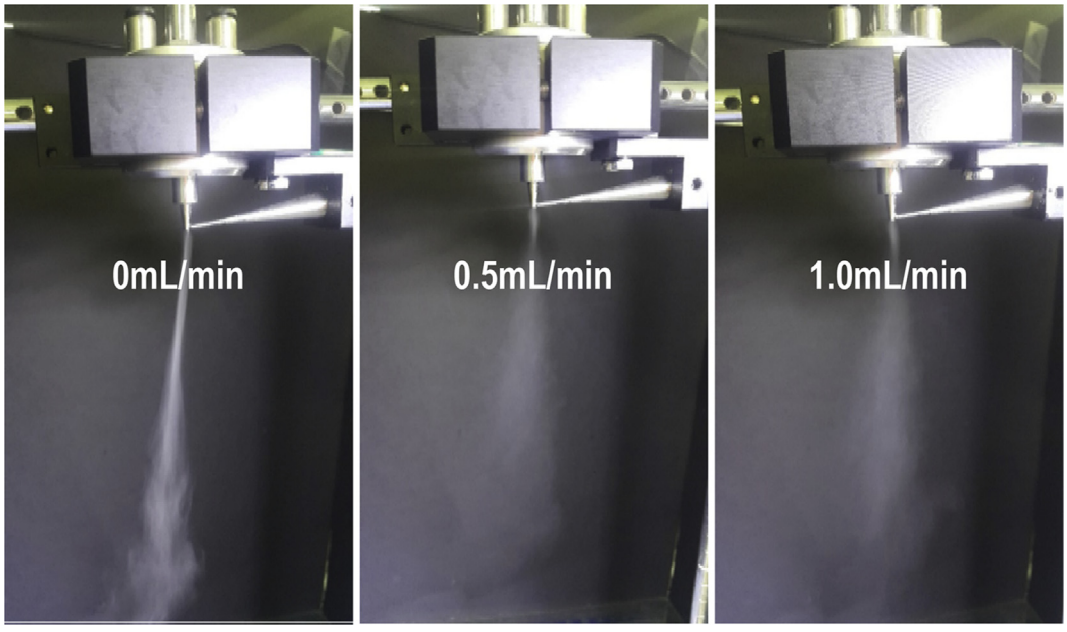


**Fig. 2.** Photographs of the US spray stream at various $N_2$ carrier gas flow rates.

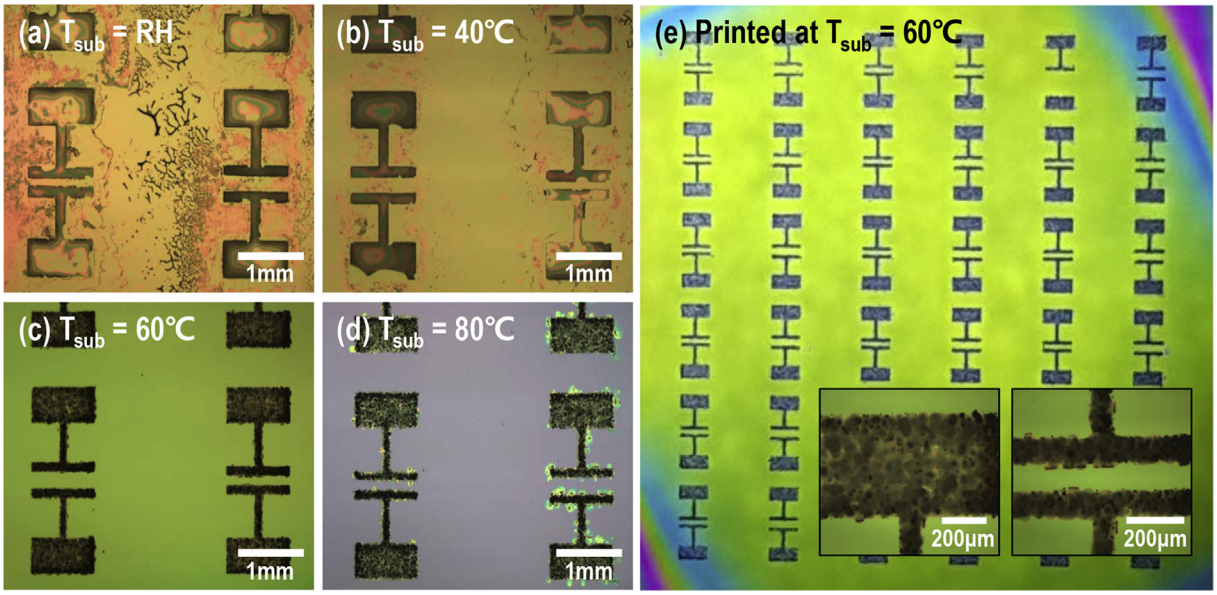


**Fig. 3.** OM images of the patterned PEDOT:PSS electrodes prepared with various substrate temperatures. **(a)** Room temperature (25 °C), **(b)** 40 °C, **(c)** 60 °C, and **(d)** 80 °C. **(e)** PEDOT:PSS electrode patterns formed by US spray printing onto a substrate 2 × 2 $cm^2$ in area heated to a substrate temperature of 60 °C. The inset images of **(e)** show enlarged OM images of the patterned PEDOT:PSS electrodes.

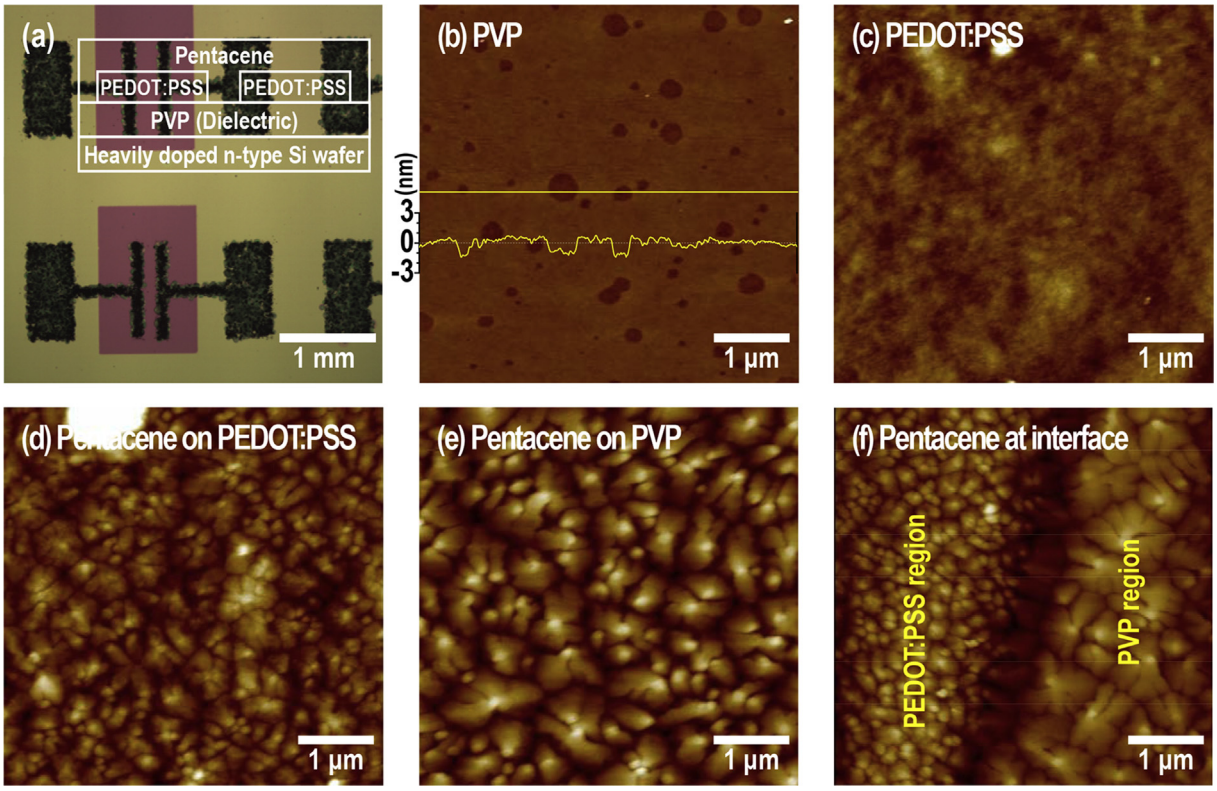


**Fig. 4.** **(a)** OM image and schematic diagram of the pentacene-FETs fabricated in this study. AFM images of **(b)** the PVP dielectric, **(c)** the PEDOT:PSS electrode, and pentacene films deposited onto **(d)** the PEDOT:PSS electrode, **(e)** PVP dielectric, and **(f)** interface region between PEDOT:PSS electrode and PVP dielectric.

700–950 nm on the PVP dielectric layer, about four-fold larger. These results could be understood in terms of differences in the surface roughness and surface energy values between the PEDOT:PSS and PVP surfaces. As mentioned above, the rms roughness of the PEDOT:PSS electrode was 1.3 nm, larger than 0.36 nm for the PVP case. The surface roughness interfered with pentacene molecular diffusion at the surface during the pentacene deposition, thereby forming a pentacene adlayer with small grains. The surface energies of the PEDOT:PSS and the PVP dielectric films were 41 and 56 $mJ/m^2$, respectively. The PVP dielectric with a high surface energy formed strong molecule–substrate interactions compared to the molecule–molecule interactions, which improved

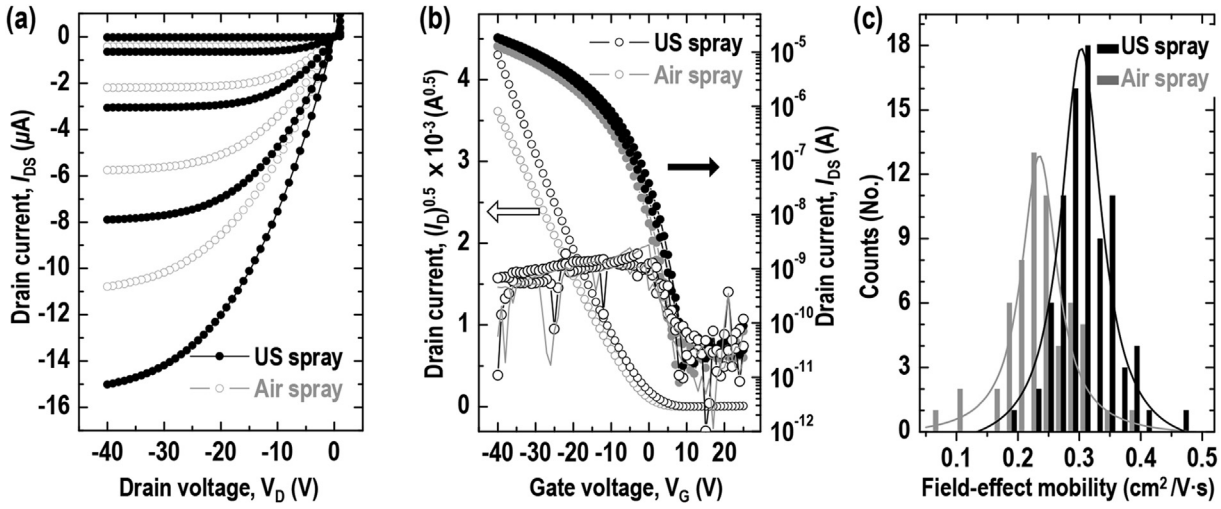


**Fig. 5.** **(a)** Output and **(b)** transfer characteristics of a pentacene-FET device fabricated from US- or air-sprayed PEDOT:PSS S/D electrodes. **(c)** Histogram of the field-effect mobilities of the pentacene-FETs prepared with PEDOT:PSS electrodes fabricated using the US (black) or air spray (gray) methods. The output and transfer characteristics of each FET were obtained with a stepped $V_G$ of −10 V and at a fixed $V_D$ of −40 V, respectively.

pentacene molecule absorption onto the surface and yielded better pentacene film structures (grain sizes or shapes) on the PVP dielectric [37,38]. The morphologies of the pentacene films deposited at the interface region of the PVP dielectric/PEDOT:PSS electrode were observed, as shown in Fig. 4(f), to have characteristics similar to those described above.

The electrical performances of the pentacene-FET devices fabricated using the air spray method were compared to confirm the superiority of the US spray method for printing PEDOT:PSS electrodes with a top-contact bottom-gate OFET structure. Fig. 5(a) shows the output characteristics of the pentacene-FETs prepared using the US or air spray methods. The devices functioned as well-behaved p-type transistors with characteristics that included a linear regime at small drain voltage ($V_D$) values and a saturation regime at $V_D$ exceeding the gate voltage ($V_G$). The FET device prepared with US-sprayed PEDOT:PSS electrodes has provided a current level that was 1.5 times the value obtained from the air-sprayed device. The transfer characteristics shown in Fig. 5(b) revealed the same electrical performance trend as the output characteristics. The on-current of the US-sprayed device was about 1.5 times the value obtained from the air-sprayed device, as described above. The transfer characteristics were used to calculate the field-effect mobility in the saturation regime using the relationship $I_{DS} = C_i\mu W(V_G - V_{th})^2/2L$, where W and L are the channel width and length, respectively, $C_i$ is the specific capacitance of the gate dielectric, $V_{th}$ is the threshold voltage, and μ is the field-effect mobility. The device-to-device reproducibility of the pentacene-FETs fabricated in our experiments was characterized by measuring the field-effect mobilities in 83 FET devices prepared using the US method and 60 FET devices prepared using the air spray method, as shown in Fig. 5(c). The pentacene-FETs prepared using the air-sprayed PEDOT:PSS electrodes showed a maximum mobility of 0.39 $cm^2V^{-1}s^{-1}$ (with an average value of 0.23 $cm^2V^{-1}s^{-1}$) and an average $V_{th}$ of −3.9 V. Application of the US spray method to the fabrication of the PEDOT:PSS electrodes enhanced the electrical performances of the pentacene-FETs up to a maximum mobility of 0.47 $cm^2V^{-1}s^{-1}$ and an average mobility of 0.31 $cm^2V^{-1}s^{-1}$ and an average $V_{th}$ of −3.7 V. The device-to-device reproducibility was improved, as indicated by the decrease in the standard deviation of the mobility values from 30% for the air spray devices to 24% for the US spray devices. The US spray method appeared to provide highly uniform PEDOT:PSS electrodes due to the generation of small droplets compared to the air spray method. These results indicated that the US spray method is better, reliable, reproducible, and promising as a method of fabricating low-cost large-area organic electronic devices.

## 4. Conclusions

In this study, we investigated the utility of the US spray method by printing PEDOT:PSS organic electrodes for the fabrications of low-cost large-area organic electronics. The US spray technique sprays a solution through ultrasonically vibrating head and nozzle parts that induce atomization of the solution. This method is advantageous in that it sprays extremely small amounts of a solution (0.2 mL/min in this study) and produces droplets a few micrometers in size compared to the conventional air spray method. The PEDOT:PSS layer was deposited using the US spraying process at several $N_2$ carrier gas flow rates and substrate temperatures. The resulting coated PEDOT:PSS electrode films were then characterized. The superiority of the US spray method was confirmed by comparing the PEDOT:PSS electrode properties with those obtained using the conventional air spray process. The pentacene-FET prepared using the US spray process showed maximum and average field-effect mobilities of 0.47 and 0.31 $cm^2V^{-1}s^{-1}$, respectively, and an average $V_{th}$ of −3.7 V. These results improved the electrical performances by about 35% compared with the performances obtained using the air spray process. Furthermore, the device-to-device reproducibility improved, as indicated by the decrease in the standard deviation of the mobility values from 30% for the air spray device to 24% for the US spray device. These results revealed that the US spray method is efficient and superior compared to the conventional air spray method for the development of low-cost large-area organic electronics.

## Acknowledgements

This work was supported by Basic Science Research Program through the National Research Foundation of Korea (NRF) funded by the Ministry of Education (NRF-2016R1D1A1B03936094).

## Appendix A. Supplementary data

Supplementary data related to this article can be found at http://dx.doi.org/10.1016/j.orgel.2017.06.061.

## References


[1] H. Klauk, Organic thin-film transistors, Chem. Soc. Rev. 39 (2010) 2643–2666.
[2] D.J. Gundlach, J.E. Royer, S.K. Park, S. Subramanian, O.D. Jurchescu, B.H. Hamadani, A.J. Moad, R.J. Kline, L.C. Teague, O. Kirillov, C.A. Richter, J.G. Kushmerick, L.J. Richter, S.R. Parkin, T.N. Jackson, J.E. Anthony, Contact-induced crystallinity for high-performance soluble acene-based transistors and circuits, Nat. Mater 7 (2008) 216–221.
[3] A.C. Arias, J.D. MacKenzie, I. McCulloch, J. Rivnay, A. Salleo, Materials and applications for large area electronics: solution-based approaches, Chem. Rev. 110 (2010) 3–24.
[4] A. Nathan, A. Ahnood, M.T. Cole, S. Lee, Y. Suzuki, P. Hiralal, F. Bonaccorso, T. Hasan, L. Garcia-gancedo, A. Dyadyusha, S. Haque, P. Andrew, S. Hofmann, J. Moultrie, D. Chu, A.J. Flewitt, G.C. Ferrari, M.J. Kelly, J. Roberson, G.A.J. Amaratunga, W.I. Milne, Flexible electronics: the next ubiquitous platform, Proc. IEEE 100 (2012) 1486–1517.
[5] P. Lin, F. Yan, Organic thin-film transistors for chemical and biological sensing, Adv. Mater 24 (2012) 34–51.
[6] S. Bisoyi, U. Zschieschang, M.J. Kang, K. Takimiya, H. Klauk, S.P. Tiwari, Bias-stress stability of low-voltage p-channel and n-channel organic thin-film transistors on flexible plastic substrates, Org. Electron 15 (2014) 3173–3182.
[7] U. Zschieschang, M.J. Kang, K. Takimiya, T. Sekitani, T. Someya, T.W. Canzler, A. Werner, J. Blochwitz-Nimoth, H. Klauk, Flexible lowvoltage organic thin-film transistors and circuits based on C10-DNTT, J. Mater. Chem. 22 (2012) 4273–4277.
[8] S.S. Lee, C.S. Kim, E.D. Gomez, B. Purushothaman, M.F. Toney, C. Wang, A. Hexemer, J.E. Anthony, Y.-L. Loo, Controlling nucleation and crystallization in solution-processed organic semiconductors for thin-film transistors, Adv. Mater 21 (2009) 3605–3609.
[9] Y.-L. Loo, Solution-processable organic semiconductors for thin-film transistors: opportunities for chemical engineers, AlChE J. 53 (2007) 1066–1074.
[10] Y.-L. Loo, I McCulloch, Progress and challenges in commercialization of organic electronics, MRS Bull. 33 (2008) 653–662.
[11] A.G. Kelly, T. Hallam, C. Backes, A. Harvey, A.S. Esmaeily, I. Godwin, J. Coelho, V. Nicolosi, J. Lauth, A. Kulkarni, S. Kinge, L.D.A. Siebbeles, G.S. Duesberg, J.N. Coleman, All-printed thin-film transistors from networks of liquid-exfoliated nanosheets, Science 356 (2017) 69–73.
[12] M. Aryal, K. Trivedi, W. Hu, Nano-confinement induced chain alignment in ordered P3HT nanostructures defined by nanoimprint lithography, ACS Nano 3 (2009), 2085–3090.
[13] S.H. Kim, K. Hong, W. Xie, K.H. Lee, S. Zhang, T.P. Lodge, C.D. Frisbie, Electrolyte-gated transistors for organic and printed electronics, Adv. Mater 25 (2013) 1822–1846.
[14] J.Y. Seok, M. Yang, A Novel blade-jet coating method for achieving ultrathin, uniform film toward all-solution-processed large-area organic light-emitting diodes, Adv. Mater. Technol. 1 (2016) 1600029.
[15] S.R. Forrest, The path to ubiquitous and low-cost organic electronic appliances on plastic, Nature 428 (2004) 911–918.
[16] R.R. Søndergaard, M. Hösel, F.C. Krebs, Roll-to-Roll fabrication of large area functional organic materials, J. Polym. Sci. Pt. B-Polym. Phys. 51 (2013) 16–34.
[17] M.M. Ling, Z. Bao, Thin film deposition, patterning, and printing in organic thin film transistors, Chem. Mater 16 (2004) 4824–4840.
[18] F. Aziz, A.F. Ismail, Spray coating methods for polymer solar cells fabrication: a review, Mat. Sci. Semicond. Proc. 39 (2015) 416–425.
[19] S.F. Tedde, J. Kern, T. Sterzl, J. Fürst, P. Lugli, O. Hayden, Fully spray coated organic photodiodes, Nano Lett. 9 (2016) 980–983.
[20] T. Fukuda, A. Sato, Fluorene bilayer for polymer organic light-emitting diode using efficient ionization method for atomized droplet, Org. Electron 26 (2015) 1–7.
[21] N.A. Azarova, J.W. Owen, C.A. Mclellan, M.A. Grimminger, E.K. Chapman, J.E. Anthony, O.D. Jurchescu, Fabrication of organic thin-film transistors by spray-deposition for low-cost, large-area electronics, Org. Electron 11 (2010) 1960–1965.
[22] U. Bielecka, P. Lutsyk, K. Janus, J. Sworakowski, W. Bartkowiak, Effect of solution aging on morphology and electrical characteristics of regioregular P3HT FETs fabricated by spin coating and spray coating, Org. Electron 12 (2011) 1768–1776.
[23] A. Abdellah, B. Fabel, P. Lugli, G. Scarpa, Spray deposition of organic semiconducting thin-films: towards the fabrication of arbitrary shaped organic electronic devices, Org. Electron 11 (2010) 1031–1038.
[24] D. Khim, K.-J. Baeg, B.-K. Yu, S.-J. Kang, M. Kang, Z. Chen, A. Facchetti, D.-Y. Kim, Y.-Y. Noh, Spray-printed organic field-effect transistors and complementary inverters, J. Mater. Chem. C 1 (2013) 1500–1506.
[25] K. Gilissen, J. Stryckers, P. Verstappen, J. Drijkoningen, G.H.L. Heintges, L. Lutsen, J. Manca, W. Maes, W. Deferme, Ultrasonic spray coating as deposition technique for the light-emitting layer in polymer LEDs, Org. Electron 20 (2015) 31–35.
[26] S. Das, B. Yang, G. Gu, P.C. Joshi, I.N. Ivanov, C.M. Rouleau, T. Aytug, D.B. Geohegan, K. Xiao, High-performance flexible perovskite solar cells by using a combination of ultrasonic spray-coating and low thermal budget photonic curing, ACS Photonics 2 (2015) 680–686.
[27] S. Liu, X. Zhang, H. Feng, J. Zhang, L. Zhang, W. Xie, Two-dimensional-growth small molecular hole-transporting layer by ultrasonic spray coating for organic light-emitting devices, Org. Electron 47 (2017) 181–188.
[28] H.–J. Lee, Y.–S. Song, T.K. An, W.–K. Choi, S.–R. Kim, Ultrasmooth transparent conductive hybrid films of reduced graphene oxide and single-walled carbon nanotube by ultrasonic spraying, Synth. Met. 221 (2016) 340–344.
[29] J.G. Tait, C. Wong, M. Turbiez, B.P. Rand, P. Heremans, Ultrasonic spray coating of 6.5% efficient diketopyrrolopyrrole-based organic photovoltaics, IEEE J. Photovolt. 4 (2014) 1538–1544.
[30] Y. Jang, Y.D. Park, J.A. Lim, H.S. Lee, W.H. Lee, K. Cho, Patterning the organic electrodes of all-organic thin film transistors with a simple spray printing technique, Appl. Phys. Lett. 89 (2006) 183501.
[31] C. Kim, A. Facchetti, T.J. Marks, Polymer gate dielectric surface viscoelasticity modulates pentacene transistor performance, Science 318 (2007) 76–80.
[32] H.S. Lee, D.H. Kim, J.H. Cho, M. Hwang, Y. Jang, K. Cho, Effect of the phase states of self-assembled monolayers on pentacene growth and thin-film transistor characteristics, J. Am. Chem. Soc. 130 (2008) 10556–10564.
[33] Y.D. Park, J.A. Lim, H.S. Lee, K. Cho, Interface engineering in organic transistors, Mater. Today 10 (2007) 46–54.
[34] H. Sirringhaus, Device physics of solution-processed organic field-effect transistors, Adv. Mater 17 (2005) 2411–2425.
[35] L.-L. Chua, P.K.H. Ho, H. Sirringhaus, R.H. Friend, Observation of field-effect transistor behavior at self-organized interfaces, Adv. Mater 16 (2004) 1609–1615.
[36] H.-G. Min, E. Seo, J. Lee, N. Park, H.S. Lee, Behavior of pentacene molecules deposited onto roughness-controlled polymer dielectrics films and its effect on FET performance, Synth. Met. 163 (2013) 7–12.
[37] J.E. Northrup, M.L. Tiago, S.G. Louie, Surface energetics and growth of pentacene, Phys. Rev. B 66 (2002) 121404.
[38] R. Ruiz, D. Choudhary, B. Nichel, T. Toccoli, K. –Chul Chang, A.C. Mayer, P. Clancy, J.M. Blakely, R.L. Headrick, S. Iannotta, G.G. Malliaras, Pentacene thin film growth, Chem. Mater 16 (2004) 4497–4508.